

RESEARCH

Open Access



Alterations in gut microbiota and host transcriptome of patients with coronary artery disease

Liuying Chen^{1†}, Xuanting Mou^{1†}, Jingjing Li^{2†}, Miaofu Li¹, Caijie Ye³, Xiaofei Gao¹, Xiaohua Liu¹, Yunlong Ma^{2,4,5*}, Yizhou Xu^{1*} and Yigang Zhong^{1*}

Abstract

Background Coronary artery disease (CAD) is a widespread heart condition caused by atherosclerosis and influences millions of people worldwide. Early detection of CAD is challenging due to the lack of specific biomarkers. The gut microbiota and host-microbiota interactions have been well documented to affect human health. However, investigation that reveals the role of gut microbes in CAD is still limited. This study aims to uncover the synergistic effects of host genes and gut microbes associated with CAD through integrative genomic analyses.

Results Herein, we collected 52 fecal and 50 blood samples from CAD patients and matched controls, and performed amplicon and transcriptomic sequencing on these samples, respectively. By comparing CAD patients with health controls, we found that dysregulated gut microbes were significantly associated with CAD. By leveraging the Random Forest method, we found that combining 20 bacteria and 30 gene biomarkers could distinguish CAD patients from health controls with a high performance (AUC = 0.92). We observed that there existed prominent associations of gut microbes with several clinical indices relevant to heart functions. Integration analysis revealed that CAD-relevant gut microbe *genus Fusicatenibacter* was associated with expression of CAD-risk genes, such as *GBP2*, *MLKL*, and *CPR65*, which is in line with previous evidence (Tang et al., *Nat Rev Cardiol* 16:137-154, 2019; Kummen et al., *J Am Coll Cardiol* 71:1184-1186, 2018). In addition, the upregulation of immune-related pathways in CAD patients were identified to be primarily associated with higher abundance of genus *Blautia*, *Eubacterium*, *Fusicatenibacter*, and *Monoglobus*.

Conclusions Our results highlight that dysregulated gut microbes contribute risk to CAD by interacting with host genes. These identified microbes and interacted risk genes may have high potentials as biomarkers for CAD.

Keywords Coronary artery disease, Gut microbe, Transcriptome, Risk genes, Biomarkers

[†]Liuying Chen, Xuanting Mou and Jingjing Li contributed equally to this study.

*Correspondence:

Yunlong Ma
myl_genomics@wmu.edu.cn

Yizhou Xu
qqyzxu@hotmail.com

Yigang Zhong
zhongyigangly@163.com

Full list of author information is available at the end of the article



Background

Coronary artery disease (CAD) mostly arising from atherosclerosis is the most common type of heart disease, which affects millions of individuals worldwide [1]. The cause of CAD is multifactorial that involve complex environmental and genetic factors [2–4]. CAD process can be effectively prevented by drug therapy, percutaneous coronary intervention (PCI), or coronary artery bypass graft (CABG) surgery [5, 6]. However, the early diagnosis of CAD remains substantially difficult due to lack of adequate biomarkers. Although several biomarkers, such as Fibrinogen and C-reactive protein, have been reported to be associated with CAD [7, 8], these biomarkers generally lack sufficient specificity and significantly detectable changes appear mainly in the advanced stages of CAD [9]. Thus, the early diagnosis and intervention of CAD pose a significant public health challenge with enormous medical and societal consequences. There is an urgent requirement for new and effective biomarkers to assist in the early diagnosis, monitoring, and management of CAD.

Gut microbiota comprises the tens of thousands of intestinal bacteria and the biological activity in the human intestine [10–13], which is essential to the development of human health [14–21]. Host-microbiota interactions, including inflammatory and metabolic processes, have been well-documented to be involved in the etiology of multiple complex diseases [22, 23]. Multiple lines of evidence have shown that the gut microbiota can influence distant cells and organs via a variety of biochemical signals or metabolites [24]. In particular, recent studies have indicated that gut microbiome potentially impact the cardiovascular system [25, 26]. An increased potential for several intestinal flora metabolites, including lipopolysaccharides [27], grammabutyrobetaine [28], and trimethyllysine [29] biosynthesis in the microbiome, has been identified among CAD patients. Most notably, a growing number of studies have linked increased levels of the gut microbe-derived trimethylamine-N-oxide (TMAO) to cardiovascular diseases [30, 31]. It has also recently been demonstrated that the composition of gut microbiota can induce the alterations in various serum metabolite concentrations that are significantly relevant to the severity of CAD [32]. Hence, integrating metagenomics with other omics approaches including transcriptomics to investigate the host-microbiome interactions will allow for distinguishing effective biomarkers and developing precision medicine for the treatment of atherosclerotic cardiovascular diseases [33, 34].

To date, investigating the contribution of gut microbiome changes to CAD is insufficient, and the mechanism underlying synergistic interactions between host genes and gastrointestinal microbes remains unclear. Thus, we

performed an integrative genomic analysis to uncover the synergy between host genes and gut microbes associated with CAD. Furthermore, we also conducted a series of bioinformatics analyses to explore the molecular functions and potential mechanisms of microbe-associated host genes for the development of CAD, and give a clue of the potential biomarkers for diagnosing CAD.

Results

Overview of gut microbiota

A total of 52 fecal and 50 blood samples from CAD patients and matched controls were sequenced in the current study (Supplementary Tables S1 and S2). Clinical information, including baseline characteristics, medications, and laboratory data of the CAD and control group, is shown in Table 1. There was no significant difference in age, gender, background medication, or other baseline characteristics between the two groups of subjects ($P > 0.05$). The degree of coronary artery stenosis was significantly different between the two groups ($P < 0.05$). At the same time, according to the results of coronary angiography, we judged that patients with CAD were in the same disease stage, that is, at least one main coronary artery stenosis $\geq 70\%$, but not AMI.

Through 16S rRNA sequencing, we obtained 964 Operational Taxonomic Units (OTUs) from all 52 fecal samples using Qiime2 software. Among them, there were 654 (67.84%) shared OTUs between CAD and control subjects, and 248 (25.73%) and 62 (6.43%) unique OTUs for CAD and control groups, respectively (Fig. 1a). Although no significant difference was observed in Shannon (Fig. 1b) and Phylogenetic Diversity (PD, Fig. 1c) indexes between CAD and control groups, beta-diversity analysis revealed that there was a significant difference in overall bacterial composition between two groups (Fig. 1d).

To provide a clearer understanding of the gut microbial features in CAD patients, we summarized the relative abundance of gut microbes at different taxonomic levels. At phylum level, the major gut microbes belong to *Firmicutes*, *Bacteroidota*, *Fusobacteriota*, and *Proteobacteria* (Fig. 1e and g). At genus level, the top 10 abundant bacteria were *Bacteroides*, *Prevotella_9*, *Lactobacillus*, *Limosilactobacillus*, *Fusobacterium*, *Ligilactobacillus*, *Escherichia-Shigella*, *Faecalibacterium*, *Klebsiella*, and *Alloprevotella* (Fig. 1f).

Difference in gut microbiota between CAD and control group

By performing differential abundant analysis, we identified 18 differential abundant genera between CAD patients and health controls (Fig. 2a and Supplementary Table S3). Genus *Blautia*, *Fusicatenibacter*, *Monoglobus*, and *Eubacterium* were depleted in CAD patients, while

Table 1 Clinical characteristics of patients with CAD and non-CAD

	CAD (n = 31)	Control (n = 23)	p
Age (years)	63.97 ± 8.33	62.28 ± 6.84	0.419
Males (n, %)	16 (51.61)	12 (52.17)	0.977
Smoker (n, %)	15 (48.39)	9 (39.13)	0.614
Alcohol (n, %)	14 (45.16)	12 (52.17)	0.713
Arterial hypertension (n, %)	18 (58.06)	16 (69.57)	0.598
Diabetes mellitus (n, %)	9 (29.03)	5 (21.74)	0.603
Hyperlipidemia (n, %)	4 (9.68)	3 (13.04)	0.989
Family history of CAD (n, %)	6 (19.35)	2 (8.70)	0.314
Syncope (n, %)	1 (3.23)	0 (0)	0.389
Atrial fibrillation (n, %)	2 (6.45)	4 (17.39)	0.233
Peripheral arterial disease (n, %)	1 (3.23)	1 (4.35)	0.832
Leukocyte (× 10 ⁹ /L)	6.26 ± 1.62	6.07 ± 1.91	0.782
Neutrophil (%)	63.14 ± 7.51	61.82 ± 9.81	0.571
Lymphocyte (%)	27.58 ± 6.57	29.08 ± 8.06	0.445
Hemoglobin (g/L)	134.77 ± 16.11	137.04 ± 15.39	0.596
Platelet (× 10 ⁹ /L)	217.94 ± 43.19	217.80 ± 60.99	0.992
Albumin (g/L)	39.03 ± 3.23	39.33 ± 2.21	0.694
ALT (U/L)	22.81 ± 11.30	18.25 ± 5.31	0.074
AST (U/L)	23.55 ± 7.27	23.63 ± 4.45	0.962
Creatinine (umol/L)	76.74 ± 18.39	73.03 ± 19.73	0.475
Uric acid (umol/L)	310.35 ± 85.91	305.35 ± 81.14	0.829
Triglyceride (mmol/L)	2.06 ± 1.87	1.53 ± 1.33	0.253
Cholesterol (mmol/L)	4.13 ± 0.87	4.21 ± 0.93	0.736
High-density lipoprotein (mmol/L)	1.05 ± 0.25	1.17 ± 0.27	0.099
Low-density lipoprotein (mmol/L)	2.17 ± 0.68	2.24 ± 0.83	0.722
CKMB (U/L)	14.26 ± 9.46	14.83 ± 4.91	0.788
cTNI (ug/L)	0.05 ± 0.14	0.01 ± 0.00	0.168
Echocardiography			
LVEF (%)	64.53 ± 4.63	63.27 ± 8.30	0.494
Medication			
ACEI (n, %)	7 (22.58)	3 (13.04)	0.421
ARB (n, %)	10 (32.26)	9 (39.13)	0.674
ARNI (n, %)	3 (9.68)	4 (17.39)	0.436
β-blocker (n, %)	24 (77.42)	12 (25.25)	0.261
Ivabradine (n, %)	0 (0.00)	2 (8.70)	0.101
MRA (n, %)	7 (22.58)	2 (8.70)	0.217
Antiplatelet drugs/A (nticoagulants (n, %)	31 (100.00)	23 (100.00)	1.000
Lipid lowering agents (n, %)	28 (90.32)	20 (86.96)	0.897
Coronary artery stenosis (%)	84.58 ± 6.58	15.71 ± 1.35	< 0.01*

* P < 0.05

Sutterella, *Lachnospiraceae_NK4A136_group*, *UCG-002*, *UCG-005*, [*Eubacterium*] *hallii_group*, *Collinsella*, *Colidextribacter*, *NK4A214_group*, *Negativibacillus*, *Faecalitalea*, *Family_XIII_AD3011_group*, *Peptoniphilus*, *Fructilactobacillus*, and *Solobacterium* were enriched in CAD patients. Among them, eight of these identified microbes, including *Blautia*, *Fusicatenibacter*,

Monoglobus, *Eubacterium*, *UCG-002*, *UCG-005*, *Collinsella*, and *NK4A214_group*, have been reported to be associated with CAD, acute myocardial infarction, or CAD complicated with non-alcoholic fatty liver disease in previous studies [27, 35–42]. For example, Hu et al. [37] reported that the decreased abundances of *Fusicatenibacter* was identified in CAD patients, and Ahrens

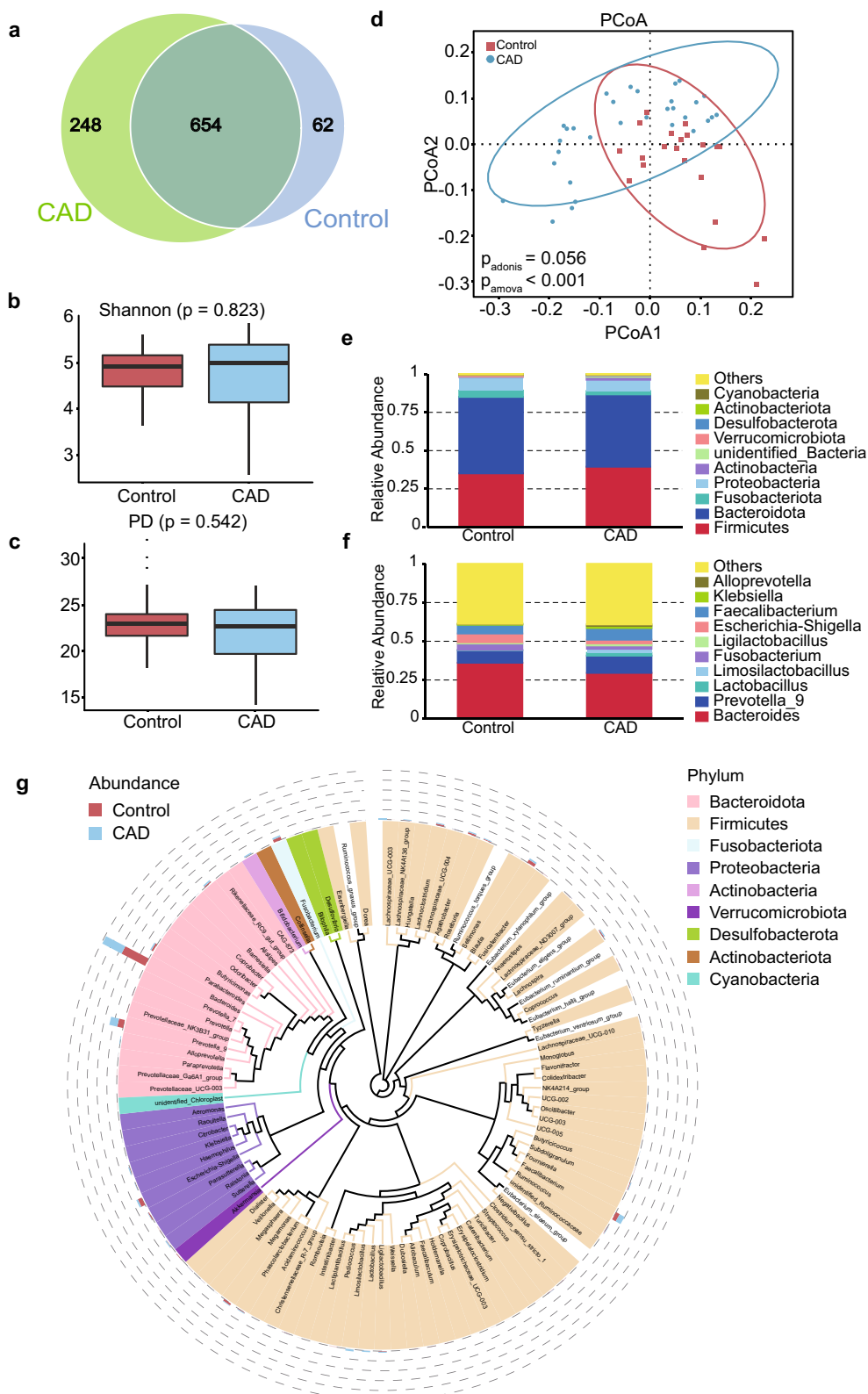


Fig. 1 Overview of intestinal flora composition in control and CAD patients. **A** OTU Difference Venn diagram between Con and CAD; The Operational Taxonomic Units (OTUs) were generated by using the Uparse. **B** and **C** The Shannon and PD indexes; **D** beta-diversity analysis; The blue circle indicates the PCoA of CAD patients, and red circle indicates that of controls. **E** and **F** the major gut microbes at phylum level; **G** the major gut microbes at genus level

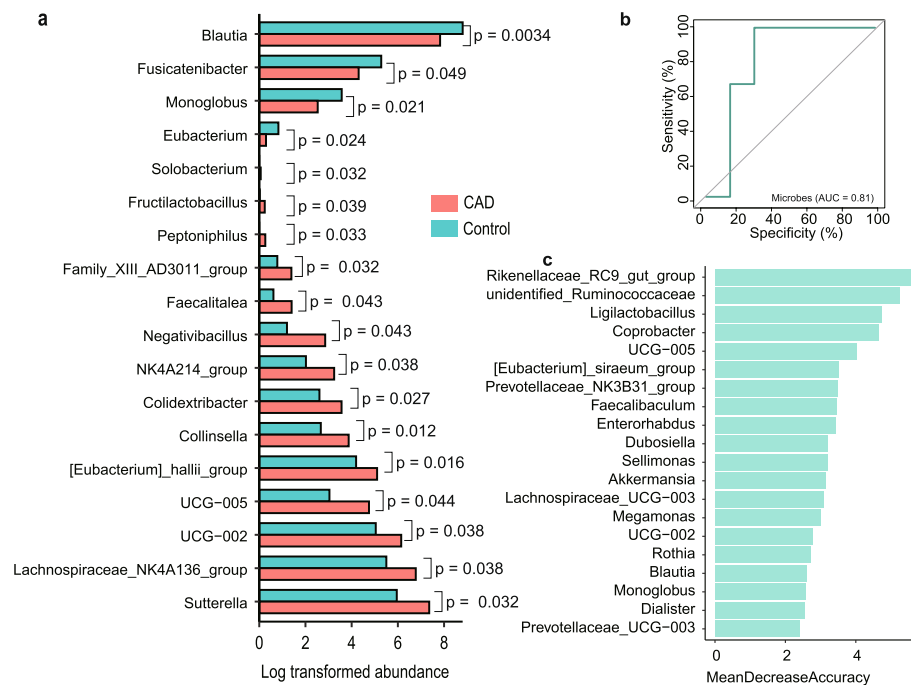


Fig. 2 Difference of gut microbiota between CAD and Control group. **A** The differential abundant genera between CAD and control group. The abundance of microbe was log-transformed. The significant level of each microbe was calculated by using Student's t-test. **B** The AUC of genus-level abundance. **C** The top 10 differential genera between CAD and control group

et al. [42] documented that *Monoglobus* was significantly decreased in CAD patients, which are in line with our findings as shown in Fig. 2a ($P=0.049$ for *Fusicatenibacter*, and $P=0.021$ for *Monoglobus*). We found that *Blautia* exhibited significantly low-abundances in CAD patients, whereas the enrichment of *Blautia* was observed in CAD patients with in-stenosis in a previous study [38]. Notably, several microbes, including *Sutterella*, *Colidextribacter*, *Negativibacillus*, *Faecalitalea*, *Peptoniphilus*, *Fructilactobacillus*, and *Solobacterium*, were identified to be associated with CAD in the current investigation (Fig. 2a). Detailed taxonomic abundance differences of gut microbiota at all taxonomic levels are shown in the Supplementary Fig. 1a-d.

By applying the Random Forest procedure, we found that 20 bacteria biomarkers can distinguish CAD patients from health controls with a good performance. The overall AUC was 0.81 using genus-level abundance as input (Fig. 2b). By overlapping genera identified from two independent methods of Mean Decrease Accuracy (Fig. 2c) and Mean Decrease Gini (Supplementary Fig. 1e), we emphasized the importance of *Rikenellaceae_RC9_gut_group*, *Coprobacter*, *Blautia*, and *Faecalibaculum* on CAD, of which several have been reported to be associated with CAD or its comorbidities [38, 43, 44]. Of note, the biomarker genus *Blautia* was also identified to be significantly differential genera.

Functional implications of gut microbiota dysbiosis in CAD

To further explore gut microbial functional dysbiosis of CAD patients, we performed functional annotation and differential analyses based on bacterial profiles. We observed a depletion of three biological pathways, including beta-Lactam resistance, cationic antimicrobial peptide (CAMP) resistance and viral proteins functions, and an up-regulation of 10 biological pathways, including nitrogen and methane metabolism, microRNAs in cancer and tropine, piperidine and pyridine alkaloid biosynthesis in CAD patients comparing with health controls ($P<0.05$, Fig. 3a and Supplementary Table S4).

Furthermore, we measured the associations of differential abundant bacteria between CAD and health groups with 23 clinical indices, including blood routine, heart, liver, and kidney functions. There were a series of significant associations between gut microbes and clinical indices relevant to heart functions. Genus *Sutterella*, *Fructilactobacillus*, and *Peptoniphilus* were positively associated with cardiac troponin I (cTNI), the cardiac regulatory proteins that control the calcium mediated interaction between actin and myosin. Brain natriuretic peptide (BNP) was significantly associated with genus *Negativibacillus*. Creatine kinase (CK) showed significantly positive correlations with genus *Fusicatenibacter*, *Blautia*, and [*Eubacterium*]*_hallii_group*. In addition, C-reactive protein (CRP) is a widely

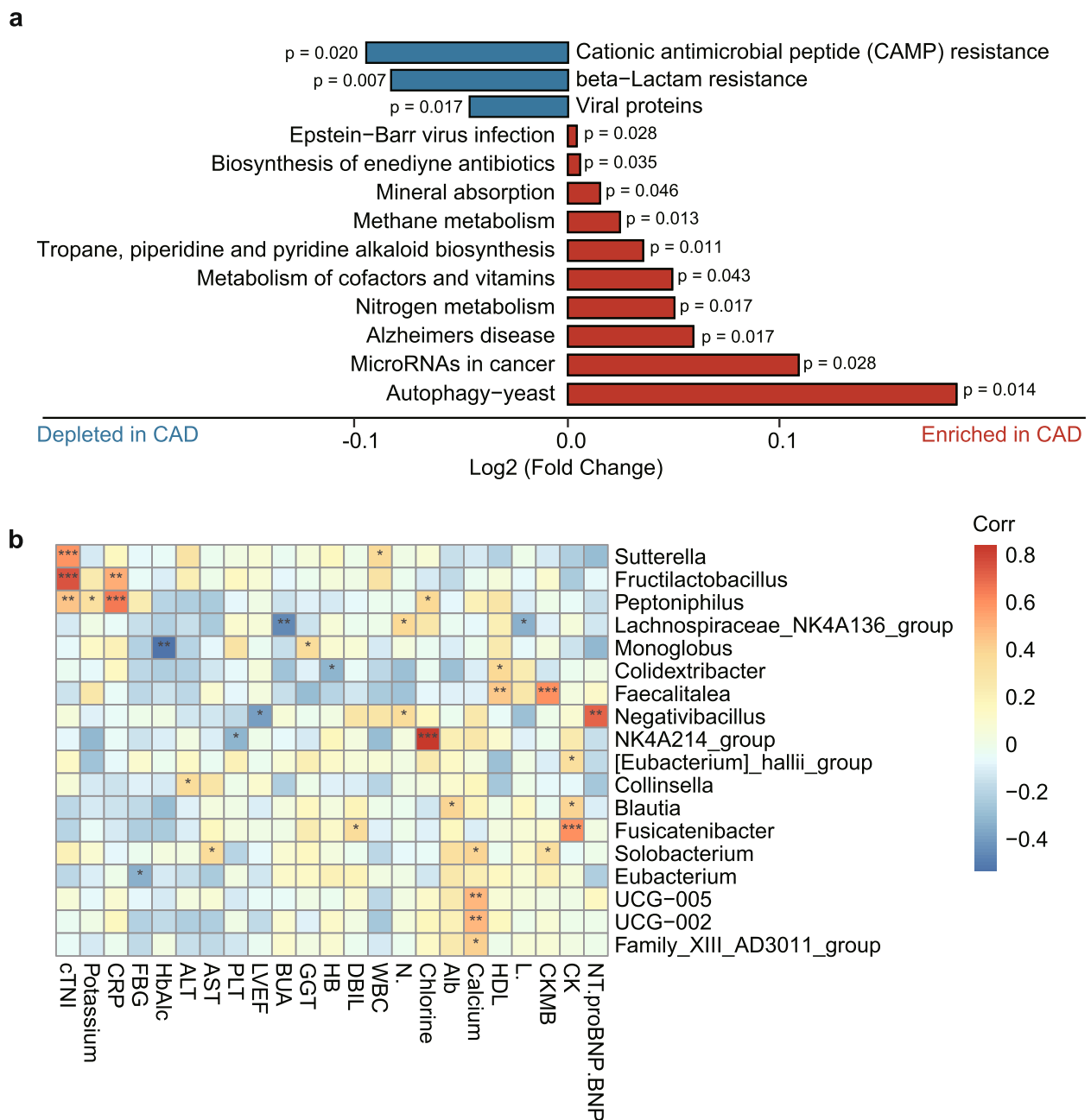


Fig. 3 Function annotation and differential analyses of gut microbiota dysbiosis. **A** Functional implications of gut microbial dysfunction in patients with CAD; The x axis indicates the log2-transformed fold change of each functional annotation. P value for each functional annotation was showed in the plot. The functional information of bacterial genomes from the KEGG database, annotated using the UProC and PAUDA methods, was mapped to the SILVA database. **B** The association of differential abundant bacteria with clinical indices. Significances tested by Pearson correlation analysis. * FDR < 0.05; ** FDR < 0.01; *** FDR < 0.001. Color bar indicates the level of correlation coefficients (corr)

used marker of inflammation [45], and elevated CRP levels are involved in the development and progression of thrombosis and CAD [46]. Our results indicate that CRP exhibit a significantly positive association with genus *Peptoniphilus* and *Fructilactobacillus* (Fig. 3b).

Transcriptional analysis revealed genes associated with gut microbes

To reveal transcriptome difference between CAD patients and health controls, we further performed differential gene expression analysis on PBMC transcriptomic

profiles. Comparing with health controls, there were 409 up-regulated and 762 down-regulated genes in CAD patients ($P < 0.05$; Fig. 4a and Supplementary Table S5), including *APOE* and *OLFML3*, which have been well-documented to be associated with CAD in previous studies [47, 48]. GSEA analysis showed that CAD group is characterized by depletion in interferon signaling-related pathways, including interferon gamma signaling pathway and interferon alpha/beta signaling pathway, and is enriched in several immune-regulated and inflammation-related pathways, including TNFs bind their physiological receptors, Rap1 signaling, and TNFR2 non-canonical NF- κ B pathway (Fig. 4b). Random Forest procedure identified that differentially expressed genes distinguished CAD patients from health controls with an AUC value of 0.84. Moreover, combining gene and microbial biomarkers increased performance of the Random Forest model, with an AUC value of 0.92 (Fig. 4c).

Considering that the significantly dis-regulated gut microbes might be associated with host gene abnormal expression and biological functions, we performed a correlation analysis on differentially abundant gut microbes ($n = 18$) and differentially expressed genes ($P < 0.01$, $n = 347$). We obtained a total of 697 suggestive or significant correlations ($P < 0.05$, Fig. 4d). Among them, there were seven significant correlations with *g_Fusicatenibacter* with FDR-adjusted $P < 0.05$, including six positively correlated genes of *GBP2*, *MLKL*, *GPR65*, *SLK*, *ETV6*, and *AFF1*, and one negatively correlated gene of *CD70* (Fig. 4e). Among these genes, several have been documented to be implicated in the development of CAD [49, 50]. For example, a network-based prioritization analysis identified the interferon-induced guanylate-binding protein 2 (*GBP2*) as a key regulator orchestrating biological processes relevant to CAD [49]. *MLKL*, which can directly induce necroptosis [51], has been reported to be involved in different inflammatory diseases, including tumor necrosis factor-induced shock [52], ischemia–reperfusion injuries [53], and obesity [54]. Recently, Kamal and coworkers have found that *MLKL* is associated to hallmarks of atherosclerosis with and without type II

diabetes mellitus, which could be a potential drug target for treating atherosclerotic patients [50]. Thus, these *g_Fusicatenibacter*-host gene interactions may play an important role in CAD.

Different gene programs associated with gut microbes

We further performed differential gene program analysis to explore whether there exist distinct gene sets with different functions associated with gut microbes. Based on the unsupervised clustering analysis, these differential genes were grouped into two clusters (Fig. 4d). Cluster 1 (highlighted in red) were positively correlated with genera that were depleted in CAD patients (e.g., *Blautia*, *Eubacterium*, *Fusicatenibacter*, and *Monoglobus*). Cluster 2 (highlighted in blue) were positively correlated with genera that were enriched in CAD patients. Pathway enrichment analysis demonstrated that genes in cluster 1 showed significant enrichments in immune-related pathways (FDR-adjusted $P < 0.05$), including regulation of *RUNX1* expression and activity, interferon gamma signaling, *DDX58/IFIH1*-mediated induction of interferon-alpha/beta and interferon signaling. This highlighted a set of genes involved in interferon signaling pathway, such as *BP2*, *GBP4*, *GBP5*, *GBP6*, *PML*, *STAT1*, *CASP10*, *IFIH1*, *TRAF6*, *UBA7*, and *UBE2L6* (Fig. 4d). Although no significant enrichment was observed for genes in cluster 2 (FDR-adjusted $P < 0.05$), we identified that several pathways exhibited suggestive enrichments for genes in cluster 2 ($P < 0.05$), including *GRB7* events in *ERBB2* signaling, sodium-coupled sulphate, di- and tri-carboxylate transporters, and *PI3K* events in *ERBB4* signaling. Together, these two distinct gene programs relevant to gut microbes potentially have different biological functions contributing to CAD.

Discussion

The role of gut microbes in CAD is still not fully understood. Deciphering correlation of gut microbes with CAD related gene functions and clinical indices contribute in understanding the underlying pathophysiological mechanism of CAD. In the current study, we performed

(See figure on next page.)

Fig. 4 The transcriptome difference between CAD and control group. **A** The volcano map of differential genes between CAD patients and controls; Red color indicates the significantly up-regulated genes, blue color indicates the significantly down-regulated genes, and gray indicates non-significant genes. **B** The pathway enrichment analysis of differential genes by using GSEA. The x axis indicates the normalized enrichment score. Dark blue or dark orange indicates FDR-adjusted P value ≤ 0.05 , and light blue or light orange indicates FDR-adjusted P value > 0.05 . **C** The ROC plot showing the performance of the combination of gene and microbial biomarkers based on Random Forest model. The blue line indicates the performance of using gene expression biomarker alone, and the red line indicates the performance of combining gene and microbial biomarker. **D** Heatmap showing the correlation analysis on differentially abundant gut microbes and differentially expressed genes. * indicates the significant correlation ($P < 0.05$). Color bar in indicate the correlation coefficient (corr). **E** Representative example demonstrating the correlation of *g_Fusicatenibacter* (log-transformed abundance) with the log-transformed expression of seven genes. There were one negatively correlated gene of *CD70* and six positively correlated genes (i.e., *AFF1*, *GPR65*, *MLKL*, *GBP2*, *SLK*, and *ETV6*)

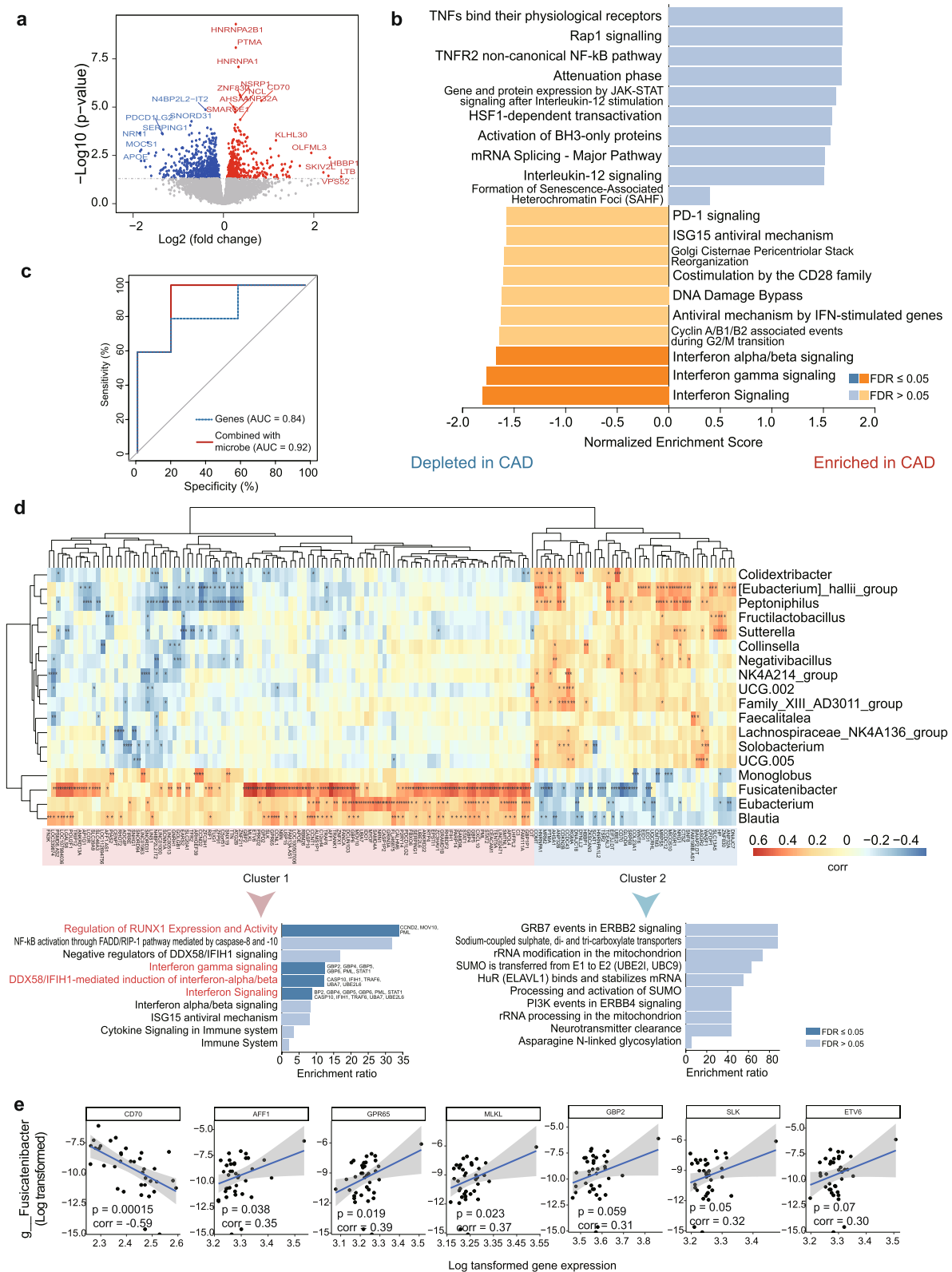


Fig. 4 (See legend on previous page.)

16S rRNA sequencing to comprehensively elucidate difference in profiles of gut microbiome in CAD patients and health controls. Our results exhibited that structure of gut microbiome differed in CAD and health group. In the CAD patients, 4 genera such as *Blautia*, *Eubacterium*, and *Fusicatenibacter* were depleted, and 14 genera such as *Sutterella*, and *Collinsella* were enriched.

Accumulating evidence has been documented that remarkably disturbed gut microbiota were detected in patients with cardiovascular diseases [25–28]. Mitra et al. [55] indicated that host microbiome associated families, such as *Porphyromonadaceae*, *Bacteroidaceae*, *Micrococcaceae*, and *Streptococcaceae*, were increased in asymptomatic atherosclerotic plaques patients than symptomatic atherosclerotic plaques patients. Based on these findings, we particularly focused on the relationship of altered *Blautia*, *Eubacterium*, and *Fusicatenibacter* with CAD. These three microbes were major producers of short chain fatty acids (SCFAs), which are important secondary metabolites capable of regulating cardiometabolic health [56, 57]. Previous studies [58, 59] have reported a reduced abundance of SCFA producers in CAD patients in different population and resolution. A recent study by Guo et al. [60] indicated that SCFA was significantly lower in AMI group than in control group. In addition, bacteria that can produce SCFA, such as *Ruminococcus* and *Bacteroides*, were significantly reduced in CAD patients [61].

Butyrate and other SCFAs produced by gut microbes serve as signaling molecules to modulate blood pressure, inflammatory responses and other metabolic functions. There are increasing evidence indicates the importance of SCFAs in regulating cardiac function [61, 62]. Considerable studies have demonstrated the parasympathetic activation effects of the SCFA propionate [61]. Park and coworkers reported that butyrate potentiates lipoteichoic acid-induced inflammasome activation through the inhabitation of histone deacetylase (HDAC) [63]. Kibbie et al. [64] have demonstrated that butyrate is able to directly reduce CD4⁺ T cell activation and proliferation via HDAC inhibition and GPR43 signaling. Recently, Zhong et al. [65] uncovered that butyrate attenuates vascular calcification, a common pathological change in cardiovascular tissues, via its dual effects on HDAC inhibition and NF κ B activation based on cellular and animal models. Also, they found that knockdown of Gpr41 could attenuated butyrate-induced vascular smooth muscle cells calcification. Zhou et al. [66] demonstrated that oral propionate supplementation improve MI therapy by parasympathetic activation based on the gut-brain axis. Moreover, a study of malonate intervention in the treatment of myocardial infarction in mice has showed that malonate enable to shift the cardiac metabolic pattern of

oxidative phosphorylation to glucose metabolic pattern and promote cardiomyocyte proliferation, hemodialysis and cardiac regeneration in adult mice after myocardial infarction [67]. Jiang et al. [68] reported that intramembranous butyrate injection improved cardiac function by promoting macrophage differentiation and inhibiting inflammation and sympathetic remodeling after myocardial infarction. Our results emphasized the importance of gut microbial functions involved in cationic antimicrobial peptide (CAMP) resistance in CAD. CAMPs are hybrid peptides playing an important role in defending against invasive bacterial infection for host. However, in addition to antimicrobial effect, CAMPs were believed to be an important link between inflammation and atherosclerotic cardiovascular disease [69]. For example, elevated plasma α -defensin is associated with an increased risk for cardiovascular morbidity [70]. PR-39, a proline-arginine-rich cationic antimicrobial peptide, has been reported to play a cardioprotective role in myocardial I/R injury through inhibition of tumor necrosis factor- α (TNF- α)-induced degradation of the NF κ B inhibitor I κ B α [71].

The correlation of gut microbiome with CAD indicated that it could be early diagnostic marker for the risk of CAD. In this study, the AUC for gut microbiome-based diagnostic RF model was 93.9%. This was supported by a previous study [39], which has reported that predictive model based on gut microbiome is able to provide a robust prediction of CAD (AUC=87.7%). Moreover, combining gut microbiome with clinical variables increased power of prediction model, generating an AUC of 90.4%. These results reinforced the capacity of gut microbiome as diagnostic biomarkers for CAD.

To investigate the interactional functions of gut microbes and host genes on CAD, we performed correlation analysis of the abundances of gut microbes and the expression levels of host genes. We observed significant reduction of interferon signaling pathways in CAD patients, as well as strong association of depleted bacteria with genes involved in interferon signaling pathways. Our result suggested that depletion of SCFA-producing bacteria (*Blautia*, *Eubacterium*, and *Fusicatenibacter*) may contribute to the decrease of interferon signaling pathways in CAD patients. One mechanism by which microbes can modulate the host disease is through regulation of cytokine signaling [72]. Interferons (IFNs) are classified into three families (type I, type II, and type III) based on sequence homology. Among them, IFN- γ is a key cytokine implicated in both innate and adaptive immunity, and studies on the involvement of IFN- γ in multiple stages of the atherosclerotic process, playing different roles, have been carried out for decades. In vitro and in vivo studies [73] have shown that IFN- γ has both pro- and anti-atherogenic properties and plays

a large role in all stages of CAD progression. Meanwhile, the type I interferons have the capacity to regulate the development or function of virtually every immune effector cell, contributing to the anti-inflammatory and anti-tumor responses, which is essential in the process of CAD [74–76].

Some limitations in the present study are warranted to comment. First, it's worth noting that the functional profiling of the gut microbiome was computationally inferred from amplicon sequencing data, and it could differ from that measured by transcriptomic sequencing techniques. According to a previous study [77], there can be significant genomic and phenotypic diversity among strains of the same species. This diversity has important implications for the ecological function of an organism, as well as the conditions required to culture it. Thus, it is impossible to reliably assess whether a microbe is “culturable” based on 16S rRNA gene sequence. Second, current study only curated a moderate sample size to establish the link between microbiome and host transcriptomic profiles for uncovering the pathology of CAD. The identified links does not imply causality but may reflect indirect discovery of causal associations. Future studies with more large-scale samples are needed to conduct for validating the identified relationships and exploring the underlying causality. Additionally, in light of multiple lines of evidence [78–83] have documented that integrating multi-omic datasets including GWAS, single-cell sequencing data, and epigenetic data contribute to uncover the molecular etiology of complex diseases. More integrative genomic analyses of microbiome with other omics are warranted for distinguishing the pathology of CAD.

Conclusions

In summary, our results provide evidence to support that gut microbes play critical roles in CAD mediated by host genes. Reduction of SCFA-producing bacteria and interferon signaling genes are associated with CAD. Depletion of SCFA-producing bacteria, e.g. *Blautia*, *Eubacterium*, and *Fusicatenibacter*, may contribute to dysfunction of interferon signaling and cardiovascular functions. These identified microbes may have potential for diagnosis or therapy of CAD.

Methods

Study participants and sample collection

In the current cross-sectional study, 31 patients with CAD and 21 healthy controls were recruited from the Department of Cardiology, Hangzhou First People's Hospital, Zhejiang University School of Medicine. This study was reviewed and approved by the Ethics Committee of Zhejiang University. The enrolled patients signed

a written informed consent form. All patients' medical history and baseline data were obtained from the electronic medical records system. To obtain high-quality samples, patients with CAD included in this study were required to meet the following criteria: 1) age >25 years and <80 years; 2) show $\geq 70\%$ stenosis in at least one major branch of the coronary artery. The healthy control group population should meet the following criteria: 1) age >45 years and <70 years; 2) all three coronary vessels $\leq 20\%$ stenosis. Besides, individuals without coronary angiography testing or with one of follow disorders, including cancer, AMI, antibiotic exposure, and any other cardiac-related disease or systemic disease were excluded.

During the hospitalization period, these 52 subjects were educated how to properly collect midcourse fecal samples to reduce the possibility of environmental bacterial contamination. One morning fasting fecal sample was taken for the first time within 24 h of admission for each patient. All fresh fecal samples were stored in $-80\text{ }^{\circ}\text{C}$ for subsequent processing and sequencing. Pre-operative blood samples for 50 of these participants were drawn and stored in PAXgene blood RNA tubes at $-80\text{ }^{\circ}\text{C}$ before further processing [84].

16S rRNA sequencing

Total genomic DNA was extracted from fecal samples. The V3-V4 region of bacterial 16S rRNA gene was amplified using primers (341F: 5'-CCTACGGGNGGCWGCAG-3', 806R: 5'-GGACTACHVGGGTWTCTAAT-3') with barcodes. The mixed PCR products were purified using the Qiagen Gel Extraction Kit (Qiagen, Germany). Sequencing libraries were generated using the TruSeq[®] DNA PCR-Free Sample Preparation Kit (Illumina, USA). The library quality was assessed using the Qubit@ 2.0 Fluorometer (Thermo Scientific) and the Agilent Bioanalyzer 2100 system. Finally, the library was sequenced on an Illumina NovaSeq 6000 platform, generating 250 bp paired-end reads.

Raw sequences were demultiplexed based on barcodes. After trimming off the barcodes and primers, paired-end sequences were assembled with FLASH (v1.2.7). The assembled raw tags were quality controlled with Fastp (v0.23.1) [85] to obtain high-quality clean tags (Supplementary Table S1). Chimeric sequences were further removed from clean tags using vsearch (v2.22.1) [86]. The filtered sequences were clustered based on 97% identity to generate Operational Taxonomic Units (OTUs). The Uparse (v7.0.1001, <http://www.drive5.com/uparse/>) method was applied to cluster the filtered sequences into OTUs at 97% identity threshold. Representative sequences were extracted and annotated with Mothur (v1.48.0) [87] and SILVA (v138.1) database [88].

The MUSCLE (v3.8.31) [89] tool was leveraged to perform sequence alignment for obtaining phylogenetic relationships of all OTU representative sequences. Finally, the data for each sample were normalized based on the sample with the lowest number of sequences by *rrarefy()* function in the *vegan* (v2.6–4) R package [90], which generates on randomly rarefied community data frame based on the given sequencing depth to remove the effects of different sample sizes. Subsequently, alpha and beta diversity analyses were based on the normalized data.

Transcriptomic sequencing

Total RNA was extracted from the isolated PBMCs using the QIAzol and miRNeasy Mini Kit (Qiagen, CA, USA). The RNA integrity (average RIN: 7.05; standard deviation (SD): 1.27, Supplementary Table S2) was tested using the Bioanalyzer 2100 system with the RNA Nano 6000 Assay Kit (Agilent Technologies, CA, USA). Poly-T oligo-attached magnetic beads were used to purify mRNA from the total RNA, which was subsequently used to establish cDNA libraries for RNA sequencing. Quality-controlled cDNA library was sequenced on Illumina Novaseq platform (Beijing, China), producing paired-end sequences (150 bp).

Raw transcriptomic sequencing data were qualified using the FastQC (<https://www.bioinformatics.babraham.ac.uk/projects/fastqc/>). Ensembl human reference genome (<http://asia.ensembl.org/info/data/ftp/index.html>, file name: Homo_sapiens.GRCh37.75.cdna.all.fa) was used for alignment and annotation. The Hisat2 (v2.0.5) tool [91] was used to establish index for reference genome, and align reads to the reference genome. The FeatureCounts (v1.5.0-p3) method [92] was used to summarize read counts for each gene.

Functional enrichment analysis

We performed differential gene expression (DGE) analysis using the DESeq2 (v1.36.0) [93] (Supplementary Table S5). *P*-values were evaluated by the Student's *t*-test [94], and multiple testing corrections were carried out using the Benjamini & Hochberg false discovery rate (FDR) method [95]. Gene set enrichment analysis (GSEA) and over representative analysis (ORA) were performed by using the WEB-based Gene Set AnaLysis Toolkit (Web-Gestalt, <https://www.webgestalt.org/>) [96]. Pathways in the Reactome database [97] were used as a reference.

Bioinformatics and statistical analyses

Qiime (v1.9.1) [98] was used to calculate alpha diversity indexes and Unifrac distance and sample clustering tree. Unifrac distance measures the evolutionary branch weight of different OTUs in the sample OTU table to assess the differences between OTUs. After obtaining the

Unifrac distance matrix, the UPGMA algorithm was used to construct a sample clustering tree. PCoA analyses was conducted with *ade4* package in R (v2.15.3). Differences in alpha diversity indexes between groups were analyzed by the Wilcoxon rank-sum test [99] in R (v2.15.3).

Tax4Fun [100] was applied to predict functional profiles. Specifically, it extracted the full-length 16S rRNA gene sequences of prokaryotic genomes from the KEGG database [101] and used the BLASTN algorithm to align them to the SILVA SSU Ref NR database [102] (with a BLAST bitscore > 1500) to establish a relevant matrix. The functional information of bacterial genomes from the KEGG database, annotated using the UProC and PAUDA methods, was then mapped to the SILVA database [88] for functional annotation. OTUs were clustered based on the SILVA database reference sequences.

Differences in log-transformed bacterial abundance and predicted functional profiles between groups were analyzed by the Student's *t*-test in R (v2.15.3), analogue to previous studies [103, 104]. Additionally, we applied the Random Forest method [105] to recognize bacterial biomarkers that classify CAD patients from health controls. R package "randomForest" (RF) was used to perform random forest classification with default "mtry" parameters. Variable importance was measured by permuting each predictor variable and measuring the decrease in model accuracy. We adopted a nested cross-validation procedure [106] in which the least important variables were sequentially removed until the mean error rate of the model reached two standard deviations above the lowest error rate. We calculated the area under the ROC curve (AUC) with the "ROCR" package [107] in R (v2.15.3). To select biomarkers, we sorted gut microbes according to their RF importance and calculated the AUC using different numbers of top gut microbes. The gut microbes with the highest AUC were selected as biomarkers.

To assess the correlations of bacterial abundances with level blood indicators and expression levels of genes in paired peripheral blood, the Pearson correlation test was applied, and FDR-adjusted *P* < 0.05 was considered to be significant. All the plots were visualized in R (v2.15.3).

Abbreviations

CAD	Coronary artery disease
TMAO	Trimethylamine-N-oxide
CAMP	Cationic antimicrobial peptide
BNP	Brain natriuretic peptide
cTNI	Cardiac troponin I
CK	Creatine kinase
CRP	C-reactive protein
SCFA	Short chain fatty acids
PBMCs	Peripheral blood mononuclear cells
DGE	Differential gene expression
FDR	False discovery rate
GSEA	Gene set enrichment analysis
ORA	Over representative analysis

KEGG The Kyoto Encyclopedia of Genes and Genomes
 AUC Area under the ROC curve

Supplementary Information

The online version contains supplementary material available at <https://doi.org/10.1186/s12866-023-03071-w>.

Additional file 1: Supplementary Table S1. Summary of sequence reads for all samples. **Supplementary Table S2.** Summary of the basic information of all RNA samples. **Supplementary Table S3.** Differential abundant analysis of 16S-seq profiles between CAD patients and controls. **Supplementary Table S4.** The results of functional annotation and differential analyses on bacterial profiles between CAD patients and controls. **Supplementary Table S5.** Differential gene expression analysis of transcriptomic profiles between CAD patients and controls.

Additional file 2: Supplementary Figure S1. Differential of gut microbiota between CAD patients and controls at class (A), order (B), family (C), and species (D) level. The abundance of microbe was log-transformed. The significant level of each microbe was calculated by using Student's t-test. (E) The top 10 differential genera between CAD and control group by means of Mean Decrease Gini.

Additional file 3: Supplementary Figure S2. The association of differential abundant bacteria with clinical indices according to different levels of order (A), family (B), and species (C). Significances tested by Pearson correlation analysis. * FDR < 0.05; ** FDR < 0.01; *** FDR < 0.001. Color bar indicates the level of correlation coefficients (corr).

Acknowledgements

We thank all participants and investigators who provide a contribution to the work.

Authors' contributions

CL, MX, and LJ conducted the experiments and wrote the article. LM, YC, GX, and LX were involved in parts of the experiments. XY, MY, and ZY conceived the hypothesis, designed the experiments, and reviewed the article. ZY and MY helped in guiding the revision. All authors reviewed and approved the final article.

Funding

This research was funded by the Hangzhou Medical and Health Technology Project (No. Z20200135), the Construction Fund of Key Medical Disciplines of Hangzhou (No. OO20200121), the National Natural Science Foundation of China (No. 32200535), and the Scientific Research Foundation for Talents of Wenzhou Medical University (No. KYQD20201001).

Availability of data and materials

Original contributions presented in the study are included in the manuscript. Detailed clinical baseline data is available at BIG Submission (BIG SUB, <https://ngdc.cncb.ac.cn/omix/preview/FQcgNvTM>, OMIX ID: OMIX004322). The raw and processed blood RNA sequencing data and fecal 16S sequencing data have been documented in the NCBI Gene Expression Omnibus (GEO) database (Accession Nos. GSE242046 and GSE242047). The codes to reproduce the analyzed results are available in a dedicated GitHub repository (https://github.com/mayunlong8989/microbiome_CAD).

Declarations

Ethics approval and consent to participate

All procedures followed were in accordance with the ethical standards of the responsible committee on human experimentation (institutional and national) and with the Helsinki Declaration of 1975 (in its most recently amended version). This study was reviewed and approved by the Ethics Committee of Zhejiang University. Informed consent was obtained from all patients included in the study.

Consent for publication

Not applicable.

Competing interests

The authors declare no competing interests.

Author details

¹Department of Cardiology, Affiliated Hangzhou First People's Hospital, Zhejiang University School of Medicine, Hangzhou, China. ²National Engineering Research Center of Ophthalmology and Optometry, Eye Hospital, Wenzhou Medical University, Wenzhou 325027, China. ³Zhejiang Chinese Medical University, Hangzhou, China. ⁴Department of Biomedical Informatics, Institute of Biomedical Big Data, Wenzhou Medical University, Wenzhou 325027, China. ⁵Oujiang Laboratory, Zhejiang Lab for Regenerative Medicine, Vision and Brain Health, Wenzhou 325101, Zhejiang, China.

Received: 11 August 2023 Accepted: 16 October 2023

Published online: 03 November 2023

References

- Gheorghide M, Sopko G, De Luca L, Velazquez EJ, Parker JD, Binkley PF, Sadowski Z, Golba KS, Prior DL, Rouleau JL, et al. Navigating the crossroads of coronary artery disease and heart failure. *Circulation*. 2006;114(11):1202–13.
- Sing CF, Stengård JH, Kardia SL. Genes, environment, and cardiovascular disease. *Arterioscler Thromb Vasc Biol*. 2003;23(7):1190–6.
- Van Der Harst P, Verweij N. Identification of 64 novel genetic loci provides an expanded view on the genetic architecture of coronary artery disease. *Circ Res*. 2018;122(3):433–43.
- Zhong Y, Chen L, Li J, Yao Y, Liu Q, Niu K, Ma Y, Xu Y. Integration of summary data from GWAS and eQTL studies identified novel risk genes for coronary artery disease. *Medicine*. 2021;100(11):e24769.
- Crea F, Liuzzo G. Pathogenesis of acute coronary syndromes. *J Am Coll Cardiol*. 2013;61(1):1–11.
- Beerens FJ, Claessen BE, Mahan M, Gaudino MFL, Tam DY, Henriques JPS, Mehran R, Dangas GD. Contemporary coronary artery bypass graft surgery and subsequent percutaneous revascularization. *Nat Rev Cardiol*. 2022;19(3):195–208.
- Behague I, Poirier O, Nicaud V, Evans A, Arveiler D, Luc Gr, Cambou JP, Scarabin PY, Bara L, Green F. β Fibrinogen gene polymorphisms are associated with plasma fibrinogen and coronary artery disease in patients with myocardial infarction: the ECTIM study. *Circulation*. 1996;93(3):440–9.
- Chen L, Yao Y, Jin C, Wu S, Liu Q, Li J, Ma Y, Xu Y, Zhong Y. Integrative genomic analysis identified common regulatory networks underlying the correlation between coronary artery disease and plasma lipid levels. *BMC Cardiovasc Disord*. 2019;19(1):1–10.
- Laaksonen R, Ekroos K, Sysi-Aho M, Hilvo M, Vihervaara T, Kauhanen D, Suoniemi M, Hurme R, März W, Schrnagl H, et al. Plasma ceramides predict cardiovascular death in patients with stable coronary artery disease and acute coronary syndromes beyond LDL-cholesterol. *Eur Heart J*. 2016;37(25):1967–76.
- Li J, Ma Y, Bao Z, Gui X, Li AN, Yang Z, Li MD. Clostridiales are predominant microbes that mediate psychiatric disorders. *J Psychiatr Res*. 2020;130:48–56.
- Ma Y, Li MD. Establishment of a strong link between smoking and cancer pathogenesis through DNA methylation analysis. *Sci Rep*. 2017;7(1):1–13.
- Cani PD. Human gut microbiome: hopes, threats and promises. *Gut*. 2018;67(9):1716–25.
- Tomofuji Y, Kishikawa T, Maeda Y, Ogawa K, Otake-Kasamoto Y, Kawabata S, Nii T, Okuno T, Oguro-Igashira E, Kinoshita M. Prokaryotic and viral genomes recovered from 787 Japanese gut metagenomes revealed microbial features linked to diets, populations, and diseases. *Cell Genomics*. 2022;2(12): 100219.
- Shreiner AB, Kao JY, Young VB. The gut microbiome in health and in disease. *Curr Opin Gastroenterol*. 2015;31(1):69.
- Yatsunenko T, Rey FE, Manary MJ, Trehan I, Dominguez-Bello MG, Contreras M, Magris M, Hidalgo G, Baldassano RN, Anokhin AP. Human gut microbiome viewed across age and geography. *Nature*. 2012;486(7402):222–7.

16. David LA, Maurice CF, Carmody RN, Gootenberg DB, Button JE, Wolfe BE, Ling AV, Devlin AS, Varma Y, Fischbach MA. Diet rapidly and reproducibly alters the human gut microbiome. *Nature*. 2014;505(7484):559–63.
17. Schmidt TSB, Raes J, Bork P. The human gut microbiome: from association to modulation. *Cell*. 2018;172(6):1198–215.
18. Yang Z, Li J, Gui X, Shi X, Bao Z, Han H, Li MD. Updated review of research on the gut microbiota and their relation to depression in animals and human beings. *Mol Psychiatry*. 2020;25(11):2759–72.
19. Xu L, Ma Y, Yuan J, Zhang Y, Wang H, Zhang G, Tu C, Lu X, Li J, Xiong Y. COVID-19 quarantine reveals that behavioral changes have an effect on myopia progression. *Ophthalmology*. 2021;128(11):1652–4.
20. Bonfiglio F, Liu X, Smillie C, Pandit A, Kurilshikov A, Bacigalupe R, Zheng T, Nim H, Garcia-Etxebarria K, Bujanda L. GWAS of stool frequency provides insights into gastrointestinal motility and irritable bowel syndrome. *Cell Genom*. 2021;1:3.
21. Villacampa EG, Larsson L, Mirzazadeh R, Kvastad L, Andersson A, Mollbrink A, Kokaraki G, Monteil V, Schultz N, Appelberg KS. Genome-wide spatial expression profiling in formalin-fixed tissues. *Cell Genom*. 2021;1(3):100065.
22. Sonnenburg JL, Bäckhed F. Diet–microbiota interactions as moderators of human metabolism. *Nature*. 2016;535(7610):56–64.
23. Chaguza C, Smith JT, Bruce SA, Gibson R, Martin IW, Andam CP. Prophage-encoded immune evasion factors are critical for *Staphylococcus aureus* host infection, switching, and adaptation. *Cell Genom*. 2022;2(11):100094.
24. Lozupone CA, Stombaugh JI, Gordon JI, Jansson JK, Knight R. Diversity, stability and resilience of the human gut microbiota. *Nature*. 2012;489(7415):220–30.
25. Buglioni A, Burnett JC Jr. A gut-heart connection in cardiometabolic regulation. *Nat Med*. 2013;19(5):534–6.
26. Trøseid M, Andersen GØ, Broch K, Hov JR. The gut microbiome in coronary artery disease and heart failure: Current knowledge and future directions. *EBioMedicine*. 2020;52: 102649.
27. Zhu Q, Gao R, Zhang Y, Pan D, Zhu Y, Zhang X, Yang R, Jiang R, Xu Y, Qin H. Dysbiosis signatures of gut microbiota in coronary artery disease. *Physiol Genomics*. 2018;50(10):893–903.
28. Koeth RA, Wang Z, Levison BS, Buffa JA, Org E, Sheehy BT, Britt EB, Fu X, Wu Y, Li L. Intestinal microbiota metabolism of L-carnitine, a nutrient in red meat, promotes atherosclerosis. *Nat Med*. 2013;19(5):576–85.
29. Li XS, Obeid S, Wang Z, Hazen BJ, Li L, Wu Y, Hurd AG, Gu X, Pratt A, Levison BS. Trimethyllysine, a trimethylamine N-oxide precursor, provides near-and long-term prognostic value in patients presenting with acute coronary syndromes. *Eur Heart J*. 2019;40(32):2700–9.
30. Senthong V, Li XS, Hudc T, Coughlin J, Wu Y, Levison B, Wang Z, Hazen SL, Tang WH. Plasma trimethylamine N-Oxide, a gut microbe-generated phosphatidylcholine metabolite, is associated with atherosclerotic burden. *J Am Coll Cardiol*. 2016;67(22):2620–8.
31. Xue H, Chen X, Yu C, Deng Y, Zhang Y, Chen S, Chen X, Chen K, Yang Y, Ling W. Gut microbially produced indole-3-propionic acid inhibits atherosclerosis by promoting reverse cholesterol transport and its deficiency is causally related to atherosclerotic cardiovascular disease. *Circ Res*. 2022;131(5):404–20.
32. Liu H, Chen X, Hu X, Niu H, Tian R, Wang H, Pang H, Jiang L, Qiu B, Chen X. Alterations in the gut microbiome and metabolism with coronary artery disease severity. *Microbiome*. 2019;7(1):1–14.
33. Asgari S, Luo Y, Huang C-C, Zhang Z, Calderon R, Jimenez J, Yataco R, Contreras C, Galea JT, Lecca L. Higher native Peruvian genetic ancestry proportion is associated with tuberculosis progression risk. *Cell Genom*. 2022;2(7):100151.
34. Sadler MC, Auwerx C, Deelen P, Kutalik Z. Multi-layered genetic approaches to identify approved drug targets. *Cell Genom*. 2023;3:100341.
35. Tang WW, Li DY, Hazen SL. Dietary metabolism, the gut microbiome, and heart failure. *Nat Rev Cardiol*. 2019;16(3):137–54.
36. Kummén M, Mayerhofer CC, Vestad B, Broch K, Awoyemi A, Storm-Larsen C, Ueland T, Yndestad A, Hov JR, Trøseid M. Gut microbiota signature in heart failure defined from profiling of 2 independent cohorts. *J Am Coll Cardiol*. 2018;71(10):1184–6.
37. Hu X, Zhou R, Li H, Zhao X, Sun Y, Fan Y, Zhang S. Alterations of gut microbiome and serum metabolome in coronary artery disease patients complicated with non-alcoholic fatty liver disease are associated with adverse cardiovascular outcomes. *Front Cardiovasc Med*. 2022;9:822282.
38. Fang C, Zuo K, Fu Y, Li J, Wang H, Xu L, Yang X. Dysbiosis of gut microbiota and metabolite phenylacetylglutamine in coronary artery disease patients with stent stenosis. *Front Cardiovasc Med*. 2022;9:589.
39. Zheng Y-Y, Wu T-T, Liu Z-Q, Li A, Guo Q-Q, Ma Y-Y, Zhang Z-L, Xun Y-L, Zhang J-C, Wang W-R. Gut microbiome-based diagnostic model to predict coronary artery disease. *J Agric Food Chem*. 2020;68(11):3548–57.
40. Liu Z, Li J, Liu H, Tang Y, Zhan Q, Lai W, Ao L, Meng X, Ren H, Xu D. The intestinal microbiota associated with cardiac valve calcification differs from that of coronary artery disease. *Atherosclerosis*. 2019;284:121–8.
41. Han Y, Gong Z, Sun G, Xu J, Qi C, Sun W, Jiang H, Cao P, Ju H. Dysbiosis of gut microbiota in patients with acute myocardial infarction. *Front Microbiol*. 2021;12: 680101.
42. Ahrens AP, Culpepper T, Saldivar B, Anton S, Stoll S, Handberg EM, Xu K, Pepine C, Triplett EW, Aggarwal M. A six-day, lifestyle-based immersion program mitigates cardiovascular risk factors and induces shifts in gut microbiota, specifically Lachnospiraceae, Ruminococcaceae, Faecalibacterium prausnitzii: a pilot study. *Nutrients*. 2021;13(10):3459.
43. Chai X, Wen L, Song Y, He X, Yue J, Wu J, Chen X, Cao Z, Qi Z. DEHP exposure elevated cardiovascular risk in obese mice by disturbing the arachidonic acid metabolism of gut microbiota. *Sci Total Environ*. 2023;875: 162615.
44. Zhou B, Wang H, Jin H, Wang L. GW29-e1224 The analysis of the diversity of the intestinal flora in patients with acute myocardial infarction. *J Am Coll Cardiol*. 2018;72(16S):C112–C112.
45. Yeh ET, Anderson HV, Pasceri V, Willerson JT. C-reactive protein: linking inflammation to cardiovascular complications. *Am Heart Assoc*. 2001;104:974–5.
46. Zheng JL, Lu L, Hu J, Zhang RY, Zhang Q, Chen QJ, Shen WF. Increased serum YKL-40 and C-reactive protein levels are associated with angiographic lesion progression in patients with coronary artery disease. *Atherosclerosis*. 2010;210(2):590–5.
47. Kolovou G, Yiannakouris N, Hatzivassiliou M, Malakos J, Daskalova D, Hatzigeorgiou G, Cariolou MA, Cokkinos DV. Association of apolipoprotein E polymorphism with myocardial infarction in Greek patients with coronary artery disease. *Curr Med Res Opin*. 2002;18(3):118–24.
48. Bos MM, de Vries L, Rensen PC, van Dijk KW, Blauw GJ, van Heemst D, Noordam R. Apolipoprotein E genotype, lifestyle and coronary artery disease: gene-environment interaction analyses in the UK Biobank population. *Atherosclerosis*. 2021;328:33–7.
49. Zhao Y, Chen J, Freudenberg JM, Meng Q, Consortium C, Rajpal DK, Yang X. Network-based identification and prioritization of key regulators of coronary artery disease loci. *Arterioscler Thromb Vasc Biol*. 2016;36(5):928–41.
50. Kamal AM, Sebak SA, Sanad EF. Mixed Lineage Kinase Domain-Like Pseudokinase (MLKL) gene expression in human atherosclerosis with and without type 2 diabetes mellitus. *Iran Biomed J*. 2021;25(4):265.
51. Weinlich R, Oberst A, Beere HM, Green DR. Necroptosis in development, inflammation and disease. *Nat Rev Mol Cell Biol*. 2017;18(2):127–36.
52. Newton K, Dugger DL, Wickliffe KE, Kapoor N, de Almagro MC, Vucic D, Komuves L, Ferrando RE, French DM, Webster J. Activity of protein kinase RIPK3 determines whether cells die by necroptosis or apoptosis. *Science*. 2014;343(6177):1357–60.
53. Newton K, Dugger D, Maltzman A, Greve J, Hedehus M, Martin-McNulty B, Carano R, Cao T, Van Bruggen N, Bernstein L. RIPK3 deficiency or catalytically inactive RIPK1 provides greater benefit than MLKL deficiency in mouse models of inflammation and tissue injury. *Cell Death Differ*. 2016;23(9):1565–76.
54. Xu H, Du X, Liu G, Huang S, Du W, Zou S, Tang D, Fan C, Xie Y, Wei Y. The pseudokinase MLKL regulates hepatic insulin sensitivity independently of inflammation. *Mol Metab*. 2019;23:14–23.
55. Mitra S, Drautz-Moses DI, Alhede M, Maw MT, Liu Y, Purbojati RW, Yap ZH, Kushwaha KK, Gheorghie AG, Bjarnsholt T. In silico analyses of metagenomes from human atherosclerotic plaque samples. *Microbiome*. 2015;3(1):1–14.
56. Liu X, Mao B, Gu J, Wu J, Cui S, Wang G, Zhao J, Zhang H, Chen W. Blautia—a new functional genus with potential probiotic properties? *Gut Microbes*. 2021;13(1):1875796.
57. Ranaivo H, Thirion F, Béra-Maillet C, Guilly S, Simon C, Sotherier M, Van Den Berghe L, Feugier-Favier N, Lambert-Porcheron S, Dussous I.

- Increasing the diversity of dietary fibers in a daily-consumed bread modifies gut microbiota and metabolic profile in subjects at cardio-metabolic risk. *Gut Microbes*. 2022;14(1):2044722.
58. Pagonas N, Seibert FS, Liebisch G, Seidel M, Giannakopoulos T, Sasko B, Ritter O, Babel N, Westhoff TH. Association of plasma propionate concentration with coronary artery disease in a large cross-sectional study. *Front Cardiovasc Med*. 2023;10:1063296.
 59. Jadoon A, Mathew AV, Byun J, Gadegbeku CA, Gipson DS, Afshiniana F, Pennathur S. Group MKTCCI: Gut microbial product predicts cardiovascular risk in chronic kidney disease patients. *Am J Nephrol*. 2018;48(4):269–77.
 60. Dong C, Yang Y, Wang Y, Hu X, Wang Q, Gao F, Sun S, Liu Q, Li L, Liu J. Gut microbiota combined with metabolites reveals unique features of acute myocardial infarction patients different from stable coronary artery disease. *J Adv Res*. 2023;46:101–12.
 61. Hu T, Wu Q, Yao Q, Jiang K, Yu J, Tang Q. Short-chain fatty acid metabolism and multiple effects on cardiovascular diseases. *Ageing Res Rev*. 2022;81:101706.
 62. Wang A, Li Z, Sun Z, Zhang D, Ma X. Gut-derived short-chain fatty acids bridge cardiac and systemic metabolism and immunity in heart failure. *J Nutr Biochem*. 2023;120:109370.
 63. Park O-J, Ha Y-E, Sim J-R, Lee D, Lee E-H, Kim S-Y, Yun C-H, Han SH. Butyrate potentiates *Enterococcus faecalis* lipoteichoic acid-induced inflammasome activation via histone deacetylase inhibition. *Cell Death Discovery*. 2023;9(1):107.
 64. Kibbie JJ, Dillon SM, Thompson TA, Purba CM, McCarter MD, Wilson CC. Butyrate directly decreases human gut lamina propria CD4 T cell function through histone deacetylase (HDAC) inhibition and GPR43 signaling. *Immunobiology*. 2021;226(5): 152126.
 65. Zhong H, Yu H, Chen J, Mok SWF, Tan X, Zhao B, He S, Lan L, Fu X, Chen G. The short-chain fatty acid butyrate accelerates vascular calcification via regulation of histone deacetylases and NF- κ B signaling. *Vascul Pharmacol*. 2022;146: 107096.
 66. Zhou M, Li D, Xie K, Xu L, Kong B, Wang X, Tang Y, Liu Y, Huang H. The short-chain fatty acid propionate improved ventricular electrical remodeling in a rat model with myocardial infarction. *Food Funct*. 2021;12(24):12580–93.
 67. Bae J, Salamon RJ, Brandt EB, Paltzer WG, Zhang Z, Britt EC, Hacker TA, Fan J, Mahmoud AI. Malonate promotes adult cardiomyocyte proliferation and heart regeneration. *Circulation*. 2021;143(20):1973–86.
 68. Jiang X, Huang X, Tong Y, Gao H. Butyrate improves cardiac function and sympathetic neural remodeling following myocardial infarction in rats. *Can J Physiol Pharmacol*. 2020;98(6):391–9.
 69. Li Y. The role of antimicrobial peptides in cardiovascular physiology and disease. *Biochem Biophys Res Commun*. 2009;390(3):363–7.
 70. Joseph G, Tarnow L, Astrup AS, Hansen TK, Parving H-H, Flyvbjerg A, Fryxell J. Plasma α -Defensin Is Associated with Cardiovascular Morbidity and Mortality in Type 1 Diabetic Patients. *J Clin Endocrinol Metab*. 2008;93(4):1470–5.
 71. Bao J, Sato K, Li M, Gao Y, Abid R, Aird W, Simons M, Post MJ. PR-39 and PR-11 peptides inhibit ischemia-reperfusion injury by blocking proteasome-mediated I κ B α degradation. *Am J Physiol Heart Circ Physiol*. 2001;281(6):H2612–8.
 72. Stefan KL, Kim MV, Iwasaki A, Kasper DL. Commensal microbiota modulation of natural resistance to virus infection. *Cell*. 2020;183(5):1312–1324.e1310.
 73. Voloshyna I, Littlefield MJ, Reiss AB. Atherosclerosis and interferon- γ : new insights and therapeutic targets. *Trends Cardiovasc Med*. 2014;24(1):45–51.
 74. Kartha VK, Duarte FM, Hu Y, Ma S, Chew JG, Lareau CA, Earl A, Burkett ZD, Kohlway AS, Lebofsky R. Functional inference of gene regulation using single-cell multi-omics. *Cell Genom*. 2022;2(9):100166.
 75. Koh KD, Bonser LR, Eckalbar WL, Yizhar-Barnea O, Shen J, Zeng X, Hargrett KL, Sun DI, Zlock LT, Finkbeiner WE. Genomic characterization and therapeutic utilization of IL-13-responsive sequences in asthma. *Cell Genom*. 2023;3(1):100229.
 76. Bossini-Castillo L, Glinos DA, Kunowska N, Golda G, Lamikanra AA, Spitzer M, Soskic B, Cano-Gamez E, Smyth DJ, Cattermole C. Immune disease variants modulate gene expression in regulatory CD4+ T cells. *Cell Genom*. 2022;2(4):100117.
 77. Steen AD, Crits-Christoph A, Carini P, DeAngelis KM, Fierer N, Lloyd KG, Cameron Thrash J. High proportions of bacteria and archaea across most biomes remain uncultured. *ISME J*. 2019;13(12):3126–30.
 78. Ma Y, Zhou Y, Jiang D, Dai W, Li J, Deng C, Chen C, Zheng G, Zhang Y, Qiu F. Integration of human organoids single-cell transcriptomic profiles and human genetics repurposes critical cell type-specific drug targets for severe COVID-19. *Cell Prolif*. 2023:e13558.
 79. Lv Y, Xu X, Wang Z, Huang Y, Ma Y, Wu M. Integrated multi-omics data analysis identifies a novel genetics-risk gene of IRF4 associated with prognosis of oral cavity cancer. *Curr Bioinform*. 2022;17(8):744–58.
 80. Ma Y, Qiu F, Deng C, Li J, Huang Y, Wu Z, Zhou Y, Zhang Y, Xiong Y, Yao Y. Integrating single-cell sequencing data with GWAS summary statistics reveals CD16+ monocytes and memory CD8+ T cells involved in severe COVID-19. *Genome Med*. 2022;14(1):16.
 81. Xiang B, Deng C, Qiu F, Li J, Li S, Zhang H, Lin X, Huang Y, Zhou Y, ORMDL3+ cholangiocytes having higher metabolic effects on primary biliary cholangitis. *J Nanobiotechnol*. 2021;19(1):406.
 82. Ma Y, Huang Y, Zhao S, Yao Y, Zhang Y, Qu J, Wu N, Su J. Integrative genomics analysis reveals a 21q22. 11 locus contributing risk to COVID-19. *Human Mol Genet*. 2021;30(13):1247–58.
 83. Ma Y, Deng C, Zhou Y, Zhang Y, Qiu F, Jiang D, Zheng G, Li J, Shuai J, Zhang Y, et al. Polygenic regression uncovers trait-relevant cellular contexts through pathway activation transformation of single-cell RNA sequencing data. *Cell Genom*. 2023;3(9): 100383.
 84. Huang Y, Luo J, Zhang Y, Zhang T, Fei X, Chen L, Zhu Y, Li S, Zhou C, Xu K. Identification of MKNK1 and TOP3A as ovarian endometriosis risk-associated genes using integrative genomic analyses and functional experiments. *Comput Struct Biotechnol J*. 2023;21:1510–22.
 85. Chen S, Zhou Y, Chen Y, Gu J. fastp: an ultra-fast all-in-one FASTQ pre-processor. *Bioinformatics*. 2018;34(17):i884–90.
 86. Rognes T, Flouri T, Nichols B, Quince C, Mahé F. VSEARCH: a versatile open source tool for metagenomics. *PeerJ*. 2016;4: e2584.
 87. Schloss PD, Westcott SL, Ryabin T, Hall JR, Hartmann M, Hollister EB, Lesniewski RA, Oakley BB, Parks DH, Robinson CJ. Introducing mothur: open-source, platform-independent, community-supported software for describing and comparing microbial communities. *Appl Environ Microbiol*. 2009;75(23):7537–41.
 88. Wang Q, Garrity GM, Tiedje JM, Cole JR. Naive Bayesian classifier for rapid assignment of rRNA sequences into the new bacterial taxonomy. *Appl Environ Microbiol*. 2007;73(16):5261–7.
 89. Edgar RC. MUSCLE: multiple sequence alignment with high accuracy and high throughput. *Nucleic Acids Res*. 2004;32(5):1792–7.
 90. Dixon P. VEGAN, a package of R functions for community ecology. *J Veg Sci*. 2003;14(6):927–30.
 91. Kim D, Paggi JM, Park C, Bennett C, Salzberg SL. Graph-based genome alignment and genotyping with HISAT2 and HISAT-genotype. *Nat Biotechnol*. 2019;37(8):907–15.
 92. Liao Y, Smyth GK, Shi W. featureCounts: an efficient general purpose program for assigning sequence reads to genomic features. *Bioinformatics*. 2014;30(7):923–30.
 93. Love MI, Huber W, Anders S. Moderated estimation of fold change and dispersion for RNA-seq data with DESeq2. *Genome Biol*. 2014;15(12):1–21.
 94. Owen DB. The power of Student's t-test. *J Am Stat Assoc*. 1965;60(309):320–33.
 95. Green GH, Diggler PJ. On the operational characteristics of the Benjamini and Hochberg False Discovery Rate procedure. *Stat Appl Genet Mol Biol*. 2007;6(1):Article27.
 96. Liao Y, Wang J, Jaehng EJ, Shi Z, Zhang B. WebGestalt 2019: gene set analysis toolkit with revamped UIs and APIs. *Nucleic Acids Res*. 2019;47(W1):W199–205.
 97. Fabregat A, Jupe S, Matthews L, Sidiropoulos K, Gillespie M, Garapati P, Haw R, Jassal B, Korninger F, May B. The reactome pathway knowledge-base. *Nucleic Acids Res*. 2018;46(D1):D649–55.
 98. Caporaso JG, Kuczynski J, Stombaugh J, Bittinger K, Bushman FD, Costello EK, Fierer N, Peña AG, Goodrich JK, Gordon JI. QIIME allows analysis of high-throughput community sequencing data. *Nat Methods*. 2010;7(5):335–6.
 99. Lam F, Longnecker M. A modified Wilcoxon rank sum test for paired data. *Biometrika*. 1983;70(2):510–3.

100. Wemheuer F, Taylor JA, Daniel R, Johnston E, Meinicke P, Thomas T, Wemheuer B. Tax4Fun2: prediction of habitat-specific functional profiles and functional redundancy based on 16S rRNA gene sequences. *Environ Microbiome*. 2020;15(1):1–12.
101. Kanehisa M, Furumichi M, Tanabe M, Sato Y, Morishima K. KEGG: new perspectives on genomes, pathways, diseases and drugs. *Nucleic Acids Res*. 2017;45(D1):D353–61.
102. Quast C, Pruesse E, Yilmaz P, Gerken J, Schweer T, Yarza P, Peplies J, Glöckner FO. The SILVA ribosomal RNA gene database project: improved data processing and web-based tools. *Nucleic Acids Res*. 2012;41(D1):D590–6.
103. Liu K, Xu Q, Wang L, Wang J, Guo W, Zhou M. The impact of diet on the composition and relative abundance of rumen microbes in goat. *Asian Australas J Anim Sci*. 2017;30(4):531.
104. Benson AK, Kelly SA, Legge R, Ma F, Low SJ, Kim J, Zhang M, Oh PL, Nehrenberg D, Hua K. Individuality in gut microbiota composition is a complex polygenic trait shaped by multiple environmental and host genetic factors. *Proc Natl Acad Sci*. 2010;107(44):18933–8.
105. Liaw A, Wiener M. Classification and regression by randomForest. *R News*. 2002;2(3):18–22.
106. Wainer J, Cawley G. Nested cross-validation when selecting classifiers is overzealous for most practical applications. *Expert Syst Appl*. 2021;182:115222.
107. Sing T, Sander O, Beerenwinkel N, Lengauer T. ROCr: visualizing classifier performance in R. *Bioinformatics*. 2005;21(20):3940–1.

Publisher's Note

Springer Nature remains neutral with regard to jurisdictional claims in published maps and institutional affiliations.

Ready to submit your research? Choose BMC and benefit from:

- fast, convenient online submission
- thorough peer review by experienced researchers in your field
- rapid publication on acceptance
- support for research data, including large and complex data types
- gold Open Access which fosters wider collaboration and increased citations
- maximum visibility for your research: over 100M website views per year

At BMC, research is always in progress.

Learn more biomedcentral.com/submissions

